

Tuning the ferromagnetism in Mn–Zn–O by intrinsic defects

This article has been downloaded from IOPscience. Please scroll down to see the full text article.

2007 J. Phys.: Condens. Matter 19 386232

(<http://iopscience.iop.org/0953-8984/19/38/386232>)

View [the table of contents for this issue](#), or go to the [journal homepage](#) for more

Download details:

IP Address: 129.252.86.83

The article was downloaded on 29/05/2010 at 05:17

Please note that [terms and conditions apply](#).

Tuning the ferromagnetism in Mn–Zn–O by intrinsic defects

A L Rosa¹ and R Ahuja²

¹ BCCMS, Bremen Universität, Otto-Hahn-Allee, NW1/FB1, 28359, Bremen, Germany

² Department of Physics, Uppsala University, Box 530, 75121, Uppsala, Sweden

E-mail: darosa@bccms.uni-bremen.de

Received 19 April 2007, in final form 14 July 2007

Published 4 September 2007

Online at stacks.iop.org/JPhysCM/19/386232

Abstract

In this work we employ density-functional theory (DFT) within the generalized-gradient approximation (GGA) to study the structural and electronic properties of Mn-doped ZnO in the presence and absence of vacancies. We find that pure Mn-doped ZnO exhibits anti-ferromagnetic behaviour for Mn concentrations smaller than 8.3%. We also show that oxygen vacancies in Mn-doped ZnO favour anti-ferromagnetism, whereas Zn vacancies stabilize the ferromagnetic behaviour.

1. Introduction

The breakthrough of semiconductor spintronics came with the discovery of ferromagnetism at temperatures as high as 110 K in Mn-doped GaAs [1]. In spite of all efforts to produce ferromagnetic Mn-doped GaAs at room temperature, the highest Curie temperatures (T_c) measured until now are 172 K in Mn-doped GaAs films [2] and 250 K in Mn delta-doped GaAs [3]. These temperatures are, unfortunately, too low for real device applications.

The frustrated attempts to produce room-temperature ferromagnetism in Mn-doped GaAs turned the attention to another class of material, the wide band gap semiconductors. Mn-doped ZnO was theoretically predicted to exhibit ferromagnetic behaviour [4], a result which was confirmed experimentally later on by Sharma *et al* [5]. However, the ferromagnetism in Mn-doped ZnO has been very controversial and is not yet completely understood. While some authors report the existence of room-temperature ferromagnetism [5, 6], others claim its absence [7]. One of the most important questions is the role of intrinsic defects on the ferromagnetic behaviour of Mn-doped ZnO. Recently, it has been suggested that the ferromagnetism in Mn-doped ZnO is not due to diluted impurities, but to the formation of secondary phases [8, 9]. Kundaliya *et al* [8] proposed that an oxygen-vacancy $\text{Mn}_{2-x}\text{Zn}_x\text{O}_{3-\delta}$ phase is responsible for the ferromagnetism at room temperature in Mn–Zn–O systems. Chemical manipulation show a strong correlation between the Curie temperature and Zn vacancies in Mn-doped ZnO [10]. Xu *et al* [11] have investigated the

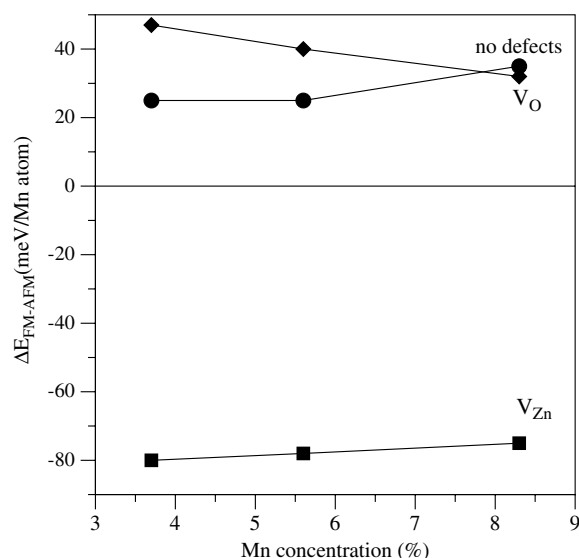


Figure 1. Total energy difference for Mn-doped ZnO as a function of the Mn concentration in the presence and absence of oxygen (V_O) and zinc (V_{Zn}) vacancies.

influence of oxygen concentration and concluded that the inclusion of free electrons by oxygen deficiency can be highly beneficial for the magnetism in ZnO. Previous calculations suggested that ferromagnetism in Mn-doped ZnO cannot be achieved without using any additional carriers [12–15].

In this work, we employ density-functional theory (DFT) to investigate the atomic, electronic and magnetic properties of Mn–Zn–O systems. We investigate the incorporation of Mn in ZnO and the influence of vacancies on their ferromagnetic stability. We show that unless intrinsic defects are present, Mn-doped ZnO exhibits an anti-ferromagnetic behaviour.

2. Computational details

We have used the projected-augmented wave (PAW) method [16] as implemented in the VASP package [17]. Exchange–correlation effects were treated within the generalized-gradient approximations (GGA) [18]. The Mn-doped ZnO supercells consisted of 48, 72 and 108 atoms. For each supercell, we replaced two Zn atoms by Mn atoms, which gives 8.3, 5.6 and 3.7% Mn concentration, respectively. The Mn atoms are aligned along the [0001] direction. The supercell lattice parameters were taken from our optimized GGA values for ZnO bulk, $a = 3.25 \text{ \AA}$ and $c = 5.35 \text{ \AA}$. We have used $(4 \times 4 \times 4)$, $(4 \times 4 \times 2)$ and $(2 \times 2 \times 2)$ \mathbf{k} -point meshes generated according to the Monkhorst–Pack scheme for the cells containing 48, 72 and 108 atoms, respectively. An energy cutoff of 500 eV was used throughout the calculations. All atoms were allowed to relax until the atomic forces were smaller than $0.001 \text{ eV \AA}^{-1}$.

3. Results

Mn replaces the Zn atoms in the ZnO lattice. To investigate the ferromagnetic stability we replace two Mn atoms in the ZnO lattice. Our calculations show that Mn incorporation in ZnO has little effect on the ZnO lattice. The Mn–O bond length differs from the Zn–O bond length by less than 0.1 \AA . Relaxations beyond first-nearest neighbours are negligible. In figure 1 we show

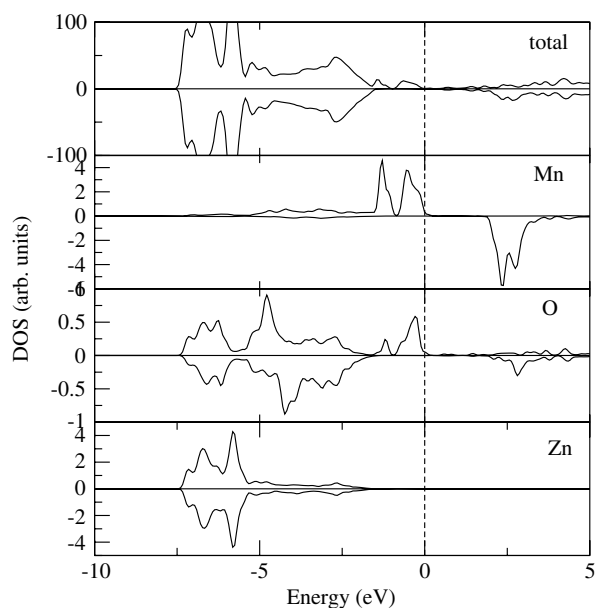


Figure 2. Total and partial density of states of Mn-doped ZnO for 5.6% Mn.

the total energy difference between the ferromagnetic (FM) and anti-ferromagnetic (AFM) configurations for pure Mn-doped ZnO. A negative value means that the FM configuration is more stable; a positive value means the opposite. We found that Mn-doped ZnO has an AFM ground state for all Mn concentrations considered here, which is in agreement with previous results [19, 12, 20]. The energy difference varies very little with the Mn concentration: it is 35 meV/Mn atom for 8.3% Mn and 25 meV/Mn atom for Mn concentrations of 3.7 and 5.6%. The same behaviour is found for the projected magnetic moments on the Mn atoms: 4.24, 4.24 and 4.29 μ_B for 3.7, 5.6 and 8.3% Mn concentration, respectively. We therefore conclude that Mn-doped ZnO in the absence of defects does not show ferromagnetic behaviour.

We have also calculated the total energy difference $\Delta E_{\text{FM-AFM}}$ between the FM and AFM configurations for Mn-doped ZnO as a function of the Mn-Mn distance. For this, we have considered a Mn concentration of 5.6% Mn. For a Mn-Mn separation of 3.27 Å, this difference is 24 meV/Mn atom. Increasing the distance to 4.62 Å and 6.52 Å reduces this difference to 2 and 1 meV, respectively. This means that the ferromagnetic interaction is short ranged. In this case a low Curie temperature is expected.

The density of states (DOS) for Mn-doped ZnO in the absence of defects in the ferromagnetic configuration is shown in figure 2. It serves as a reference point and it will permit us to discuss the differences introduced by the presence of defects. When Mn is introduced in the ZnO lattice, it replaces the zinc atoms. The Mn d shell remains half-filled, and therefore Mn doping does not introduce carriers. The exchange splitting is much larger than the crystal-field splitting, which favours Mn in the high-spin state. Therefore, in the absence of defects, the system shows an insulating behaviour, with the spin-up channel completely occupied and the spin-down channel empty. The Mn 3d states are located on the top of the valence band and strongly hybridize with the O 2p states.

Recent experiments with Mn-Zn-O have shown a correlation between magnetization and carrier concentrations [10, 11]. In order to investigate how defects influence the magnetic

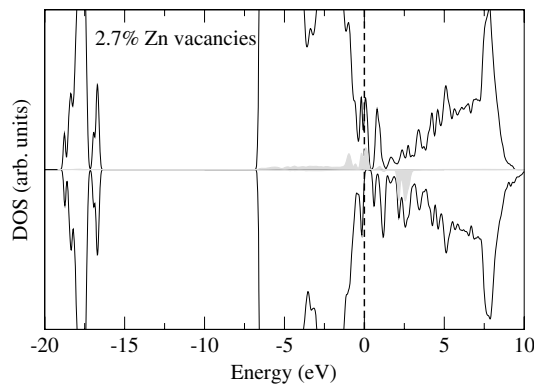


Figure 3. Total and partial density of states of Mn-doped ZnO for 5.6% Mn and 2.7% Zn vacancies. The shaded area shows the density of states projected on the Mn atom. The Fermi level is set to zero.

properties of Mn-doped ZnO, we have also considered vacancies. The defects with lowest formation energy in ZnO are O vacancies, Zn vacancies and Zn interstitials [21, 22]. Under O-rich conditions, the Zn vacancies have the lowest formation energy, whereas under Zn-rich conditions the formation of O vacancies is favoured. Because we are using supercells for our calculations, by changing the Mn concentrations, the oxygen and zinc vacancy concentrations also change. However, the range of vacancy concentration is small (2–4%) and should not affect the general conclusions.

We have chosen two possible site location for the vacancies: one with the O vacancy between the Mn atoms and another one with the O vacancy as far as possible from the Mn impurities. In the case of Zn vacancies, we removed Zn atoms as far as possible from the Mn atoms. Again, two Mn atoms per supercell were considered, in the configuration where they are second-nearest neighbours. The Mn atoms are aligned along the [0001] direction. The total energy difference between the FM and AFM configurations as a function of the Mn concentration is shown in figure 1.

In the case of oxygen vacancies, the lowest energy configuration is found if the O vacancy is located between the Mn atoms. Similar results have been found for Cu-doped ZnO [23]. By adding O vacancies, the AFM configuration is more favoured than the FM one. For example, for a Mn concentration of 3.7% and oxygen vacancy concentration of 1.8%, the energy difference between the FM and AFM configuration is 40 meV/Mn when the O vacancy is far from the Mn impurity and 61 meV/Mn when the O vacancy is close to the Mn impurities. The change in the magnetic moments compared to pure Mn-doped ZnO is also negligible: $4.21 \mu_B/\text{Mn}$ for both close and far configurations. As a general behaviour, the oxygen vacancies have little effect on the electronic structure of pure Mn-doped ZnO. Our results are in agreement with previous calculations [13–15].

On the other hand, adding Zn vacancies to Mn-doped ZnO makes the system strongly ferromagnetic. For example, adding 2.7% Zn vacancies stabilizes the ferromagnetism by 85 meV/Mn atom. The total magnetic moment decreases to $4 \mu_B$ per Mn atom and $3.6 \mu_B$ on the Mn atoms. The DOS of Mn-doped ZnO with 2.7% Zn vacancies is shown in figure 3. When Zn vacancies are introduced, the Fermi level shifts upwards, leaving the top of the valence band partially occupied. We should mention that the vacancy concentrations studied here are perhaps much larger than the ones found experimentally. Investigations for more realistic concentrations are under way.

Now we would like to address the use of the local (spin) density approximation (L(S)DA) in treating Mn-doped ZnO. It is well known that the L(S)DA might lead to a wrong description in the description of d and f electrons. Because in the L(S)DA calculations all electrons are treated as itinerant, this leads to narrow bands near the Fermi level in the case of localized electrons and does not correspond to experimental reality. One way of improving this picture is to use the L(S)DA + U approach [24]. In the GGA or L(S)DA approach, as shown above, the Mn 3d states form narrow bands. The exchange splitting, around 2 eV, is much larger than the crystal-field splitting. In order to verify the validity of the L(S)DA/GGA, we have performed GGA + U calculations for Mn-doped ZnO, varying U between 2 and 5 eV and $J = 1$ eV. We should mention that we have not performed calculations for systems involving defects and it is not possible to say how L(S)DA/GGA + U performs in this case. For this, a more systematic study is needed. In the GGA + U calculations, the Hubbard U makes the splitting between the filled and empty Mn 3d states larger. This splitting is now 3.5 eV and the crystal-field splitting is 0.8 eV. However, the anti-ferromagnetic configuration remains more stable than the ferromagnetic one, but the energy difference between both configurations decreases to 10 meV/Mn for 5.6% Mn concentration.

In summary, we have used density-functional theory to study the role of vacancies in the structural, electronic and magnetic properties of Mn-doped ZnO. We have found that oxygen vacancies in Mn-doped ZnO favour anti-ferromagnetism, whereas Zn vacancies stabilize the ferromagnetic behaviour. We believe that our results can be useful in understanding the existing controversy of ferromagnetism in Mn-doped ZnO.

Acknowledgments

We would like to thank the Swedish Foundation for International Cooperation in Research and Higher Education (STINT) for financial support and the High Performance Computing Center North, in Umeå, where most of these calculations were performed.

References

- [1] Ohno H 1998 *Science* **281** 951
- [2] Edmonds K W, Boguslawski P, Wang K Y, Novikov S N, Farley N R S, Campion R P, Neumann A C, Foxon C T, Gallagher B L, Sawiski M, Dietl T, Buongiorno Nardelli M and Bernholc J 2004 *Phys. Rev. Lett.* **92** 037201
- [3] Nazmul A M, Amemiya T, Shuto Y, Sugahara S and Tanaka M 2005 *Phys. Rev. Lett.* **95** 017201
- [4] Dietl T, Ohno H, Matsukura F, Cibert J and Ferrand D 2000 *Science* **287** 1019
- [5] Sharma P, Gupta A, Rao K V, Ahuja R, Guillen J M O, Johansson B and Gehring G A 2003 *Nat. Mater.* **2** 673
- [6] Theodoropoulou N, Misra V, Philip J, LeClair P, Berera G P, Moodera J S, Satpati B and Som T 2006 *J. Magn. Mater.* **300** 407
- [7] Rao C N R and Deepak F L 2005 *J. Mater. Chem.* **15** 573
- [8] Kundaliya D C, Ogale S G, Lofland S E, Dhar S, Metting C J, Shinde S R, Ma Z, Varughese B, Ramanujachary K V, Salamanca-Riba L and Venkatesan T 2004 *Nat. Mater.* **3** 709
- [9] Garcia M A, Ruiz-Gonzalez M L, Quesada A, Costa-Kramer J L, Fernandez J F, Khatib S J, Wennberg A, Caballero A C, Martin-Gonzalez M S, Villegas M, Briones F, Gonzales-Calbet J M and Hernando A 2005 *Phys. Rev. Lett.* **94** 217206
- [10] Kittilstved K R, Norberg N S and Gamelin D R 2006 *Phys. Rev. Lett.* **94** 147209
- [11] Xu X H, Blythe H J, Ziese M, Behan A J, Neal J R, Mokhtari A, Ibrahim R M, Fox A M and Gehring G A 2006 *New J. Phys.* **8** 135
- [12] Spaldin N A 2004 *Phys. Rev. B* **69** 125201
- [13] Sato K and Katayama-Yoshida H 2001 *Japan. J. Appl. Phys.* **40** L485
- [14] Sato K and Katayama-Yoshida H 2002 *Phys. Status Solidi* **229** 673
- [15] Iusan D, Sanyal B and Eriksson O 2006 *Phys. Status Solidi* **204** 53
- [16] Bloechl P 1994 *Phys. Rev. B* **50** 17953

-
- [17] Kresse G and Furthmüller J 1996 *Phys. Rev. B* **54** 11169
- [18] Perdew J P 1991 *Electronic Structure of Solids* ed P Ziesche and H Eschrig (Berlin: Akademie)
- [19] Sluiter M H F, Kawazoe Y, Sharma P, Inoue A, Raju A R, Rout C and Waghmare U V 2005 *Phys. Rev. Lett.* **94** 187204
- [20] Yoon S W, Cho S B, We S C, Yoon S, Suh B J, Song H K and Shin Y J 2003 *J. Appl. Phys.* **93** 7879
- [21] van de Walle C G and Neugebauer J 2004 *J. Appl. Phys.* **95** 3851
- [22] Oba F, Nishitani S R, Isotani S, Adachi H and Tanaka I 2001 *J. Appl. Phys.* **90** 824
- [23] Ye L-H, Freeman A J and Delley B 2006 *Phys. Rev. B* **73** 033203
- [24] Anisimov V I, Aryasetiawan F and Lichtenstein A I 1997 *J. Phys.: Condens. Matter* **9** 767